Vol. 376: 143–151, 2009
doi: 10.3354/meps07817

MARINE ECOLOGY PROGRESS SERIES
Mar Ecol Prog Ser

Published February 11

Eating your competitor: functional triangle between turbulence, copepod escape behavior and predation from mussels

Anders Jonsson, Torkel Gissel Nielsen*, Ivan Hrubenja, Marie Maar, Jens Kjerulf Petersen

National Environmental Research Institute, Department of Marine Ecology, University of Aarhus, Frederiksborgvej 399, 4000 Roskilde, Denmark

ABSTRACT: Clearance on different stages of the calanoid copepod *Acartia tonsa* by blue mussels *Mytilus edulis* was measured at different turbulence intensities. Turbulence enhanced consumption of all stages of the calanoid copepod *A. tonsa* by the benthic suspension feeder *M. edulis*, although with significant ontogenetic differences. Clearance on eggs increased significantly with turbulence; without turbulence, eggs sank to the bottom of the experimental cylinder and became unavailable to the mussels. In general, adult copepods escaped a filtrating mussel better than nauplii and copepodites. Experiments showed that the presence of copepodites and adult copepods reduced mussel clearance rate. The present study documents the interaction between turbulence and mussel predation on copepods and illustrates the potential of benthic suspension feeders in shaping the pelagic food web.

KEY WORDS: Turbulence · Benthic–pelagic coupling · Copepod escape response · Copepod mortality

INTRODUCTION

Pelagic copepods and benthic suspension feeders, such as mussels, are considered the most important grazers on pelagic primary producers. In the deep open ocean, copepods often have the grazing capacity to control pelagic primary production (Verity & Smetacek 1996). However, in shallow coastal localities, populations of benthic suspension feeders have the potential to clear the water column above them several times a day and thereby control the primary producers (Cloern 1982). In shallow coastal waters without strong stratification, benthic suspension feeders and copepods compete for prey. Most research has focused on the grazing impact of copepods and bivalves on primary producers, but other studies have documented that blue mussels *Mytilus edulis* are capable of ingesting copepods up to 1.2 mm in length (Kimmerer et al. 1994, Davenport et al. 2000, Wong et al. 2003). If mussels are capable of ingesting zooplankton such as copepods, they will not only have a direct source of nutrition, but also remove their major competitors from the water column. Several studies have suggested this pathway, and it has been pointed out that copepods may act as a food source for mussels, especially in turbulent environments (Horsted et al. 1988, Kim Wong 1996, Nielsen & Maar 2007, Maar et al. 2007).

Copepods possess effective escape responses. If they detect a hydromechanical signal, they will escape with a few vigorous jumps away from the signal (Hwang & Strickler 2001, Green et al. 2003, Titelman & Kiørboe 2003). During this escape copepods are measured to jump up to 200–400 body lengths per second (Buskey & Hartline 2003), eliciting one of the greatest work output per gram of muscle measured in the animal kingdom (Lenz et al. 2000). Laboratory experiments by

*Corresponding author. Email: tgn@dmu.dk

Kiørboe et al. (1999) show that adult copepods *Acartia tonsa* respond to smaller hydromechanical signals than their naupliar stages under still-water conditions, suggesting an ontogenetic refinement of the nervous system from nauplii to adult. Combined with the adult's stronger swimming capacity, this will result in a higher mortality due to mussel predation in the early stages (Kiørboe et al. 1999). In a turbulent environment, mixing of the water counteracts the escape jumps directed away from the mussel's inhalant opening. In addition, turbulence interferes with the siphonal current field, causing a decrease of the detection distance relative to the stimuli, which may result in a delayed or no escape response (Kiørboe et al. 1999, Gilbert & Buskey 2005, Waggett & Buskey 2007). Thus, copepods are more likely to be cleared by mussels under turbulent conditions.

The aim of the present study was to investigate how turbulence influences the escape success of different ontogenetic stages of the copepod *Acartia tonsa* when exposed to the benthic suspension-feeding mussel *Mytilus edulis* and turbulence intensities ranging from calm water up to a hurricane event. Because later stages of *A. tonsa* exhibit better escape responses than earlier stages, the clearance rate by *M. edulis* is predicted to decrease with copepod size. Additionally, increased turbulence should decrease escape success of *A. tonsa*

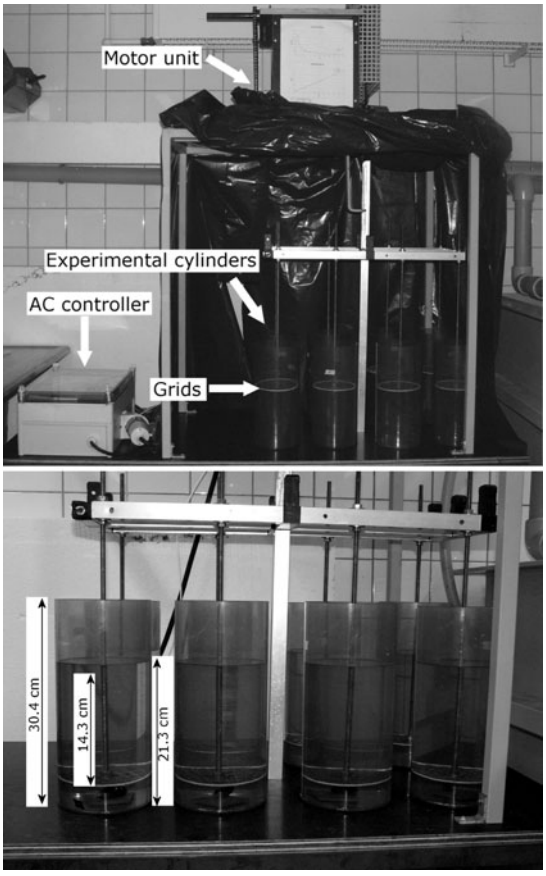

Fig. 1. Experimental setup. Top: Overview. Bottom: Close-up of experimental cylinders. Total cylinder height was 31.4 cm, water column height was 21.3 cm and stroke length was 14.3 cm, reaching 5.2 cm above the bottom and 1.8 cm below the surface

MATERIALS AND METHODS

Experiments were conducted at the National Environmental Research Institute in Roskilde, Denmark. *Mytilus edulis* were collected from the nearby Roskilde and Holbæk Fjords and kept at room temperature. They were continuously supplied with an algae culture of *Rhodomonas salina* of ~5000 cells ml^{-1}. The average shell length of the experimental mussels was 4.4 ± 1.0 cm. A laboratory culture of *Acartia tonsa* was established from eggs originating from cultures at the Danish Institute for Fisheries Research in Charlottenlund, Denmark (Støttrup et al. 1986). *R. salina* originated from the Marine Biological Laboratory in Helsingør, Denmark, were cultured at 15°C and frequently diluted with B media (Hansen 1989).

Experimental design. The experimental setup was similar to the one used by Saiz & Kiørboe (1995). Experimental containers consisted of 8 semi-clear PVC cylinders (h = 30.4 cm, mean diameter [Ø] = 13.4 cm). Turbulence was generated by means of vertical oscillating stainless steel grids (Ø = 13.2, mesh size 1 cm, open area 67%). The amplitude of the stroke was 14.3 cm, ranging from 5.2 cm above the bottom to 1.8 cm below the water surface (Fig. 1). The speed of the grids was adjusted using an AC controller (Dinverter SE) connected to a motor unit (Leroy Somer 250W). The weighted-average turbulent energy dissipation rate, ε (cm^2 s^{-3}), in the cylinders made by the grids was previously estimated at various stroke frequencies using particle tracking ((Kiørbe & Saiz 1995, Saiz & Kiørboe 1995), and we applied these estimations to the present study. The applied dissipation rates varied from 10^{-5} to 10^{-1} cm^2 s^{-3} (Table 1), falling within the range of reported dissipation rates in the upper mixed layer (Maar et al. 2003). Calm water was defined as having a dissipation rate of 10^{-5} cm^2 s^{-3}.

Mixing time in the experimental cylinders is related to dissipation rate and was measured in order to estimate the turbulent diffusivity for use in the model (Eq. 4, see below). This was measured by monitoring the spread of a neutral buoyant glass sphere suspension (NorTek seeding material) at different turbulence intensities. Three ml of the suspension was slowly added to the bottom near the wall of the cylinder using

Table 1. Grid speeds used in the experiments and the calculated turbulent dissipation rates (ε). Values are presented with the equivalent wind speeds required in nature to produce the dissipation rates (Kiørboe & Saiz 1995), and their meteorological classifications

Turbulence level	Grid speed (cm s^{-1})	ε (cm^2 s^{-3})	Wind speed (m s^{-1})	Meteorological classification
Low	0	10^{-5}	Calm	Calm
	0.19	5.2×10^{-5}	1.5	Light air
Intermediate	0.32	2.4×10^{-4}	2.5	Light breeze
	0.44	6.7×10^{-4}	3.5	Gentle breeze
	0.63	2.0×10^{-3}	5.1	Gentle breeze
	0.95	6.6×10^{-3}	7.8	Moderate breeze
High	1.90	5.4×10^{-2}	16.2	Near gale
	3.80	4.3×10^{-1}	33.3	Hurricane

a pipette, and samples were taken at regular intervals in the diagonal top end of the cylinder. The concentration of glass particles in the samples was measured with a turbidimeter (Hach 2100AN) until a steady concentration was reached (Fig. 2). It was not possible to monitor mixing time in the cylinders without grid movement since it was dependent on the mussels' orientation in the experimental cylinder and filtration activity, and therefore impossible to reproduce. Mussel biomixing in cylinders without grid movement was measured by monitoring the *Rhodomonas salina* concentration above an active filtrating mussel at 0, 10 and 20 cm above the bottom.

Four experimental cylinders (1 to 4) during all experiments contained 1 mussel each, and an additional 4 cylinders (5 to 8) served as controls. During experiments, all cylinders were filled with 3 l of 0.2 µm filtered seawater (FSW, salinity = 30 ± 1, 19.1 to 20.7°C) giving a water column height of 21.3 cm. All experiments with nauplii, copepodites and adults were run in darkness to avoid any effects of light on swimming behaviour. Clearance F (l h^{-1}) was defined as the volume of water V (l) cleared of particles and/or prey per unit of time t (h), and calculated using the modified Frost formula according to Kiørboe et al. (1982):

$$F = \frac{V}{N_m \times t} \ln\left(\frac{exp_1 \times con_2}{con_1 \times exp_2}\right) \quad (1)$$

where N_m is the number of mussels, exp_1 and exp_2 are start and end concentrations in each experimental cylinder, respectively, and con_1 and con_2 represent the average start and end concentration, respectively, of all control cylinders. Shell lengths of the experimental mussels, l_{exp} (mm), were measured before starting each experiment. Prior to data analysis, clearance rate was normalized to that of a standard mussel with a shell length of 35 mm, F_{35mm} (l h^{-1}), as:

$$F_{35mm} = \left(\frac{35}{l_{exp}}\right)^b \times F_{exp} \quad (2)$$

where F_{exp} (l h^{-1}) represents the measured clearance rate by the experimental mussel and the exponent b = 2.14 (Kiørboe & Møhlenberg 1981).

Effects of turbulence on *Mytilus edulis* clearance rate. First, we tested the effect of turbulence on *M. edulis* clearance rate of *Rhodomonas salina*. A culture of *R. salina* was added to the cylinders to achieve a concentration of 5000 cells ml^{-1}. One mussel was introduced to each experimental cylinder and turbulence was initiated. The mussels were observed to ensure that they started to filter (t_0). Every 10 min, a 10 ml sample was taken from each of the cylinders and raw fluorescence was measured on a Turner Designs 10AU fluorometer. Every 20 min, the *R. salina* concentration was adjusted to the initial concentration. The experiment was terminated after 60 min, and clearance rate was calculated for the time intervals 0–20 min and 40–60 min using Eq. (1). Total mean clearance was calculated for the 4 experimental cylinders.

Next, we tested the impact of turbulence on *Mytilus edulis* clearance rate of negatively buoyant particles using *Acartia tonsa* eggs. Prior to experiments, eggs were frozen to avoid hatching. *Rhodomonas salina* were added to the experimental cylinders to achieve an algal concentration of 5000 cells ml^{-1}. One mussel was then introduced to each of the 4 experimental cylinders. When the mussels started to filter, *A. tonsa* eggs were added to each cylinder at the surface, giving an average concentration of ~70 eggs l^{-1}, and the experiment was initiated. At t_{30}, the *R. salina* concentration was restored to the initial concentration. At t_{60}, the experiment was terminated. The contents were rinsed out of each of

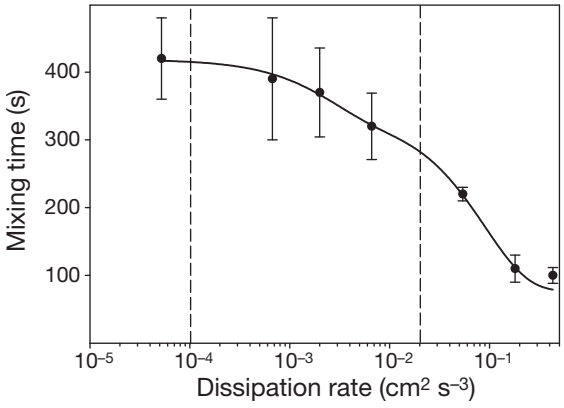

Fig. 2. Mean (±SE) time of total mixing of neutral buoyant cellulose particles versus turbulent dissipation rates. Mixing time was described as a non-linear function $f(x)$ of dissipation rate, x, given as: $f(x) = y_0 + a\exp(-bx) + c\exp(-dx)$, where y_0 = 76.76, a = 85.11, b = 395, c = 257, d = 11.04 (n = 19, R^2 = 0.78, $p < 0.05$). Dashed vertical lines: borders of low, intermediate and high turbulence

Table 2. *Rhodomonas salina* and *Acartia tonsa*. Mean (±SE) size, volume and carbon content of the species used in the experiments. Carbon content was calculated from values in the literature. Early nauplii to adult stage *A. tonsa* size calculated as prosome length

Species	Size (µm)	Volume (µm^3)	C content (µg)
R. salina	7.0 ± 0.1	180 ± 8	28.8×10^{-6} [b]
A. tonsa eggs	80.8 ± 0.4	2.76×10^5	0.04 ± 0.001[c]
A. tonsa early nauplii	114.1 ± 1.6[a]	–	0.02 ± 0.001[d]
A. tonsa late nauplii	208.6 ± 3.3[a]	–	0.19 ± 0.01[d]
A. tonsa early copepodite	354 ± 11[a]	–	0.31 ± 0.06[d]
A. tonsa adult	856 ± 31[a]	–	4.1 ± 0.4[d]

[a]Prosome length; [b]Ptacnik (2003); [c]Gorokhova (2003); [d]Berggreen et al. (1988)

the experimental cylinders and concentrated using a 30 µm filter into a petri dish; the remaining eggs were counted using a dissection microscope (10 to 40× magnification). During counting, the petri dishes were checked for pseudofeces. *M. edulis* clearance on the eggs was calculated as described above using Eq. (1).

Finally, we tested the effects of turbulence on the clearance rate of *Mytilus edulis* offered different stages of *Acartia tonsa*. Early naupliar stages were obtained by suspending eggs in aerated FSW for 24 to 30 h. Late nauplii and early copepodites were obtained by suspending eggs in aerated FSW and subsequently observed to determine when the stages under consideration were reached. After 24 h, the copepods were fed *Rhodomonas salina* on a daily basis to optimize the development into late nauplii and early copepodites. Adult *A. tonsa* were obtained from continuous 100 l batch culture.

Copepods of the stage under consideration (Table 2) were transferred to a 500 ml bottle and split using a 5 ml Vogel pipette to achieve a concentration in the experimental cylinders of ~100 ind. l^{-1}. An expected adult copepod clearance rate of *Rhodomonas salina* of 0.8 ml h^{-1} ind.$^{-1}$ (Berggreen et al. 1988) was used to correct the measured clearance rate and to ensure that only the effect of mussel clearance was considered. Nauplii and copepodite clearance on *R. salina* in the experimental cylinders was considered as being insignificant and was not investigated further. Raw fluorescence was measured in the experimental cylinders at t_0, t_{20}, t_{40} and t_{60}, and experiments with inactive mussels were discarded. The experiments were conducted as described above for *Acartia tonsa* eggs. During counting, petri dishes were checked for pseudofeces.

To illustrate the relationship between *Mytilus edulis* filtration activity and the escape response of *Acartia tonsa*, an escape coefficient was defined as:

$$\frac{F_{Rho}}{F_{Acar}} \quad (3)$$

where F_{Rho} and F_{Acar} are the individual mussel's clearance rate of *Rhodomonas salina* and *A. tonsa*, respectively. An escape coefficient of 1 indicates that *A. tonsa* and *R. salina* were cleared with the same rate and that no copepods entering the mussel's inhalant siphon escaped. The higher the escape coefficient, the more copepods escaped.

Individual-based model. To further estimate the required speed for successful escapes of *Acartia tonsa* (e.g. escape coefficients >1) exposed to mussels at different turbulence levels, we used a 1D individual-based model (IBM) describing the plankton's vertical motion in a turbulent environment and their removal by mussels. The IBM has previously been applied to explain observed distributions of plankton above a mussel bed in a Danish fjord (Maar et al. 2007) and we therefore modified the model according to the present experimental conditions. The modified model domain corresponded to the height of the water column in the experimental cylinders, and simulation time was 2 h. Turbulent diffusivity, K (cm^2 s^{-1}), in the containers was estimated from the measured mixing time t (s) and the diagonal length L = 25.2 cm of the container and assumed to be constant with depth in the model:

$$K = \frac{L^2}{t} \quad (4)$$

It was not possible to estimate K in experiments without grid movement. The behavioural components of the zooplankton motion in the model were: (1) swimming behaviour and (2) escape jumps triggered at a critical detection distance above the mussel. Zooplankton swimming behaviour was described as non-directional random zooplankton swimming, i.e. 'biodiffusion' D (m^2 s^{-1}), constant over the water column and given by this formula (Berg 1983):

$$D = \frac{u^2 \times \tau}{3} \quad (5)$$

where u (m s^{-1}) is typical swimming speed and τ (s) is average tumbling time between changes in random swimming directions as obtained from the literature (Table 3). At a critical detection distance above the mussel, *Acartia tonsa* performed escape jumps with maximum jump velocity, W_{max} (cm s^{-1}, Table 3), in the direction upwards and away from the inhalant flow. The critical detection distance was constant in the model because previous simulations showed that critical detection distance had little impact on mussel clearance rate (CR, l h^{-1}) under turbulent conditions (Maar et

al. 2007, their Fig. 10). Mussel filtration velocities in the model were calculated from the maximum mussel clearance rate, CR_{max}, and exhalant and inhalant siphon radius according to Maar et al. (2007). CR_{max} for a 4.4 cm mussel was 4.7 l h^{-1} obtained from the experiments on *Rhodomonas salina*, and the radius of exhalant and inhalant siphons was 0.25 and 0.50 cm, respectively (Newell et al. 2001), rescaled to the present shell length using an exponent of 2 (O'Riordan et al. 1995).

The IBM simulated the change in the vertical position for each individual from z_n to z_{n+1} over a finite time step, δt = 1 s, according to:

$$z_{n+1} = z_n \pm v_m \delta t + R_1 \{2r^{-1}[K(z_n) + D]\delta t\}^{1/2} \quad (6)$$

The second term is the mussel filtration velocity, v_m, assigned to be exhalant or inhalant by the ratio 1:8 (Maar et al. 2007). The third term is the turbulent diffusivity K (Eq. 4) (Table 4) and biodiffusivity D (Eq. 5), both multiplied by a random function R_1, which generates a uniform distribution between –1 and 1, and divided by a constant r = ⅓ (Visser 1997). The upper boundary was reflective, while individuals crossing the lower flux boundary were transferred to a random depth in the water column, keeping the number of individuals constant in the model. The model calculated the number of encounters, E (no. h^{-1}), between mussels and zooplankton per unit time from the total encounters in the model (all individuals crossing the lower boundary), multiplied by the percent cover of mussels on the bottom in the experiments, α. The α-value of 4% was estimated in simulations of *Rhodomonas salina* using D = 0.004 $cm^2 s^{-1}$ (Broglio et al. 2001) with no escape responses at the lowest turbulence level by fitting the modelled CR to the observed CR_{max}. CR of zooplankton was estimated from E, α and the abundance N = 388 ind. l^{-1} of zooplankton and water volume V = 3 l in the cylinders:

$$CR = MIN\left(CR_{max}, \frac{E \times V \times \alpha}{N}\right) \quad (7)$$

where CR could not exceed CR_{max}. Modelled escape coefficients were estimated according to Eq. (3) and compared to those based on observations for different life stages of *Acartia tonsa*. The model was run in Matlab (version 7.3.0.267).

Statistical analyses. Differences between groups were calculated using 1-way ANOVA and Tukey's post-hoc test. Pearson's correlation tested independence of the variables, and dissipation rate was log-transformed on the x-axis. Both methods were used with 95% confidence limits.

Table 3. *Acartia tonsa*. Sinking velocity and tumbling time of nauplii and copepodite stages CI–CVI used to calculate biodiffusion in Eq. (5), and the critical detection distance of *A. tonsa* exposed to mussel filtration (based on the literature)

	Sinking velocity (cm s^{-1})	Tumbling time (s)	Biodiffusion ($cm^2 s^{-1}$)	Detection distance (cm)
Nauplii	0.03[a]	0.033[a]	0.0001	0.56[c]
Copepodites	0.58[b]	0.1[b]	0.0112	0.77[c]

[a]Titelmann & Kiørboe (2003); [b]Jonsson & Tiselius (1990), [c]Kiørboe et al. (1999)

RESULTS

Turbulence effect on *Mytilus edulis* clearance rate

The normalized clearance rate of *Rhodomonas salina* by *Mytilus edulis* was unaffected by turbulence (Fig. 3a) and was significantly uniform across all tested dissipation rates (1-way ANOVA, $p > 0.05$), with an average value of 2.9 ± 0.1 l h^{-1}. In the experiments with adult copepods and early copepodites, the mussels' clearance rates on *R. salina* were significantly lower (1-way ANOVA, $p < 0.05$) compared with clearance in experiments with nauplii and *R. salina* alone (Table 5). Mussel clearance on *Acartia tonsa* eggs was dependent on turbulence (Fig. 3b), and showed a significantly lower normalized clearance rate at low turbulence (1-way ANOVA, $p < 0.05$) compared with intermediate and high turbulence levels, where the clearance rate was more or less constant.

Effect of turbulence on the escape success of *Acartia tonsa* from *Mytilus edulis*

Turbulence and developmental stage had a significant effect on the ability of *Acartia tonsa* to escape an actively filtering mussel (Fig. 4). All tested stages showed a decline in escape coefficients as an inverse relation to dissipation rates, while adult copepods had

Table 4. Measured mixing time in the cylinders and estimated turbulent diffusivity K (Eq. 4) used in the individual-based model (IBM) at the applied dissipation rates

Dissipation rate ($cm^2 s^{-3}$)	Mixing time (s)	K ($cm^2 s^{-1}$)
5.2×10^{-5}	420	1.51
6.7×10^{-4}	357	1.77
6.6×10^{-3}	340	1.86
5.4×10^{-2}	226	2.80
1.8×10^{-1}	120	5.28
4.3×10^{-1}	100	6.33

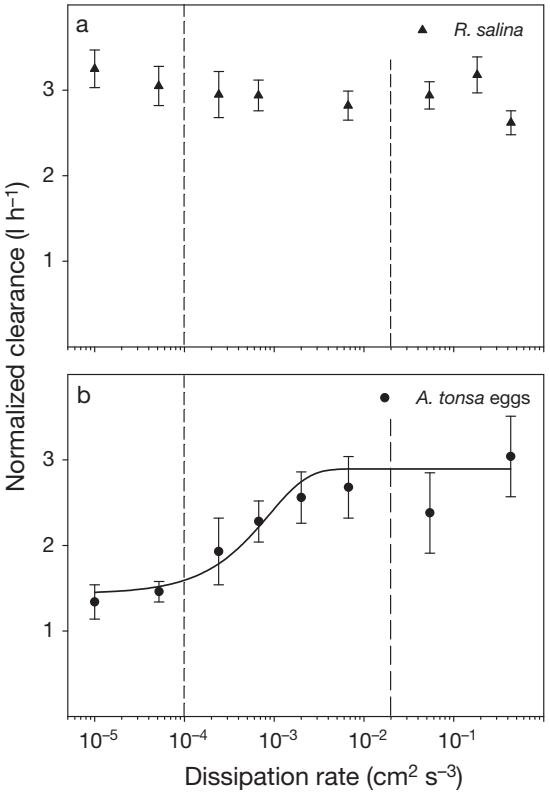

Fig. 3. *Mytilus edulis*. Mean (±SE) normalized clearance rate of *M. edulis* feeding on (a) *Rhodomonas salina* and (b) *Acartia tonsa* eggs versus turbulent dissipation rates. Normalized clearance rate of eggs was described as a non-linear function $f(x)$ of dissipation rate, x, given as: $f(x) = y_0 + a\exp(-bx)$, where $y_0 = 2.89$, $a = -1.46$, $b = 1142$ (n = 47, $R^2 = 0.26$, $p < 0.05$). Dashed vertical lines: borders of low, intermediate and high turbulence

Table 5. Normalized clearance rates of *Mytilus edulis* feeding on *Rhodomonas salina* in experiments without copepods and with nauplii, copepodite and adult stages of *Acartia tonsa*

Experiment	Clearance rate (l h^{-1})	SE	n
No copepods	2.9	0.1	237
Early nauplii	3.0	0.1	58
Late nauplii	3.1	0.1	64
Early copepodite	1.9	0.1	36
Adult	2.2	0.1	64

a significantly higher escape coefficient than younger stages at all turbulence levels (1-way ANOVA, $p < 0.05$). No pseudofaeces were found in any of the cylinders, illustrating that all copepods removed from the water column were ingested by mussels. Escape coefficients for early and late nauplii were similar and reached a maximum of about 2 at low turbulence and decreased significantly to about 1 at intermediate and high turbulence levels ($p < 0.05$) (Table 6, Fig. 4a,b).

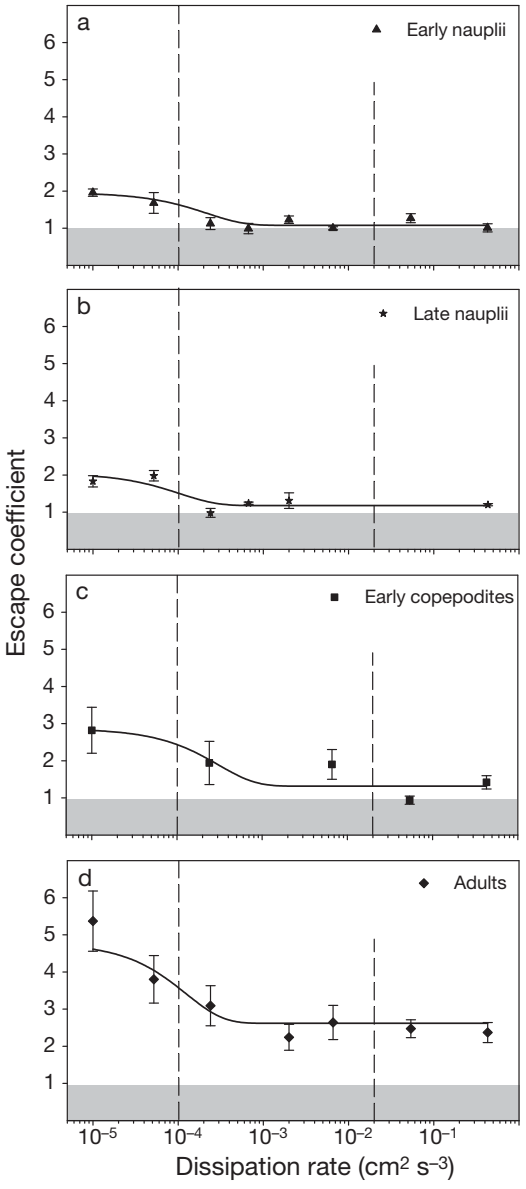

Fig. 4. *Acartia tonsa*. Mean (±SE) escape coefficients for different stages: (a) early nauplii, (b) late nauplii, (c) early copepodites, and (d) adults versus turbulent dissipation rates. Escape coefficients were described as a non-linear function $f(x)$ of dissipation rate, x, given as: $f(x) = y_0 + a\exp(-bx)$, where (a) $y_0 = 1.08$, $a = 0.88$, $b = 4575$ (n = 29, $R^2 = 0.66$, $p < 0.05$); (b) $y_0 = 1.18$, $a = 0.87$, $b = 9557$ (n = 21, $R^2 = 0.51$, $p < 0.05$); (c) $y_0 = 1.32$, $a = 1.55$, $b = 3248$ (n = 17, $R^2 = 0.26$, $p < 0.05$); and (d) $y_0 = 2.62$, $a = 2.16$, $b = 8058$ (n = 23, $R^2 = 0.39$, $p < 0.05$). Dashed vertical lines: borders of low intermediate and high turbulence levels; gray filled area: escape coefficient of 1

Escape coefficients of early copepodites were significantly higher than for nauplii at intermediate turbulence ($p > 0.05$), while there was no significant difference between these stages at high and low turbulence levels ($p > 0.05$) (Table 6, Fig. 4a–c). Adult *A. tonsa*

Table 6. *Acartia tonsa*. Escape coefficients (±SE) for nauplii, early copepodite and adult stages at low, intermediate and high turbulence

Experiment	Escape coefficient		
	Low	Intermediate	High
Early nauplii	1.7 ± 0.1	1.1 ± 0.1	1.1 ± 0.1
Late nauplii	1.6 ± 0.1	1.3 ± 0.1	1.2 ± 0.0
Early copepodites	2.8 ± 0.6	2.0 ± 0.3	1.1 ± 0.1
Adults	4.1 ± 0.6	2.3 ± 0.3	2.4 ± 0.2

could escape mussel filtration at all tested dissipation rates, and the escape coefficient of 4.5 at low turbulence was significantly higher than for intermediate and high turbulence levels ($p > 0.05$), where the escape coefficients were ~2.4 (Table 6, Fig. 4d).

Biomixing

There was no significant depletion of algae with depth (0, 10 and 20 cm) above an actively filtering mussel over time (1-way ANOVA, $p < 0.05$), showing that the mussels' filtration mixed the entire water column without grid-generated turbulence. Escape coefficients in calm water were thus not due to copepods being situated in an unmixed upper layer, but were either the result of an escape response or upwards swimming.

Modeling results

The IBM clearly showed that the escape coefficient increased with decreasing dissipation rates (Fig. 5). The escape coefficients were similar to those observed for early and late nauplii at escape speeds of 2 to 3 cm s^{-1} (Fig. 5a) and for early copepodites at escape speeds of 3 cm s^{-1} (Fig. 5b). Escape coefficients reached up to 4.8 at the highest escape speed of 5 cm s^{-1} in the model (Fig. 5b), in accordance with observations for adults at the lowest turbulence level. However, observed escape coefficients stabilized around 2.5 for adults at low dissipation rates, while modelled escape coefficient decreased gradually towards 1 with increasing dissipation rates.

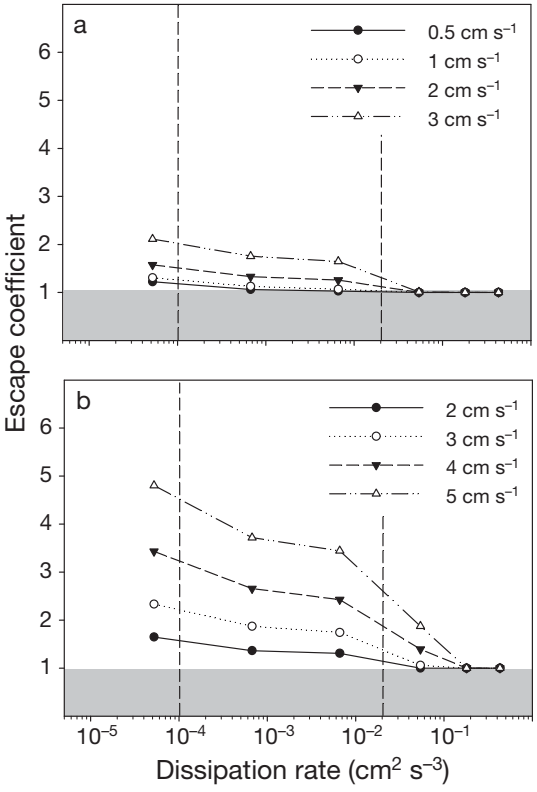

Fig. 5. *Acartia tonsa*. Average modeled escape coefficients for (a) nauplii and (b) copepodites and adults versus turbulent dissipation rates and at different escape speeds of varying from 0.5 to 5 cm s^{-1}. Dashed vertical lines: borders of low, intermediate and high turbulence; gray filled area: escape coefficient of 1. Error bars are not shown because SE was <1% of the mean

DISCUSSION

The present study demonstrated that turbulence significantly decreased the copepods' ability to detect and escape an actively filtering mussel, and that there was an ontogenetic change in the copepods' escape success in agreement with our hypothesis. In the experiments, adult copepods were the only stage that managed to escape even at the highest tested turbulence intensity, and the escape coefficients for adults were significantly higher than for nauplii and early copepodites at all tested turbulence intensities. We found no significant difference in escape coefficients between early and late nauplii, although previous studies found that late nauplii *Acartia tonsa* were slightly more sensitive in detecting a filtrating mussel than early nauplii in calm water (Kiørboe et al. 1999, Green et al. 2003). The modelled escape speeds for nauplii and early copepodites were 2 to 3 cm s^{-1}, corresponding to about 100 body lengths s^{-1} and thus in agreement with previous observations (Titelman & Kiørboe 2003). For adults, the modelled escape speed was about 4 cm s^{-1}, corresponding to 50 body lengths s^{-1}, and it was therefore easier for adults than for earlier stages to escape, due to their more sensitive detection ability and larger size. However, at high turbulence levels, observed escape coefficients for adults never dropped to 1 as expected, but stabilized around 2.5. This could be

explained by a prosome length (856 µm) close to the upper end of the retention spectrum of *Mytilus edulis*. This would also explain the discrepancy between laboratory and model results, where the escape coefficients in the model gradually decreased to 1 for all stages. Previous laboratory experiments have also demonstrated that turbulence has a negative effect on copepods' escape behaviour (Gilbert & Buskey 2005, Waggett & Buskey 2007), and that the depletion of copepods increased during high turbulence in the field (Maar et al. 2007). In conclusion, the present study documented for the first time turbulence-enhanced mortality of pelagic copepods solely caused by suspension-feeding bivalves. This interaction is of major importance for the dynamics of coastal copepod populations, as well as the nutrition of shallow water bivalve populations.

Copepods are of crucial importance for the transport of nutrients from lower to higher tropic levels (Azam et al. 1983). Field experiments estimating mussel stomach content or zooplankton depletion and laboratory grazing experiments have confirmed that mussels are capable of ingesting copepods (Horsted et al. 1988, Kimmerer et al. 1994, Wong et al. 2003, Lehane & Davenport 2002, Nielsen & Maar 2007). Mussels have both direct and indirect benefits from eating copepods. As shown in the present study, mussels remove the copepods from the water column and thereby directly benefit from their nutritional value. An indirect advantage is that the mussels eliminate their main food competitors from the water column. These interactions between zooplankton and mussels are very important to consider when, for example, establishing floating mussel rafts or bottom cultures, because mussel grazing may have significant impacts on the zooplankton community (Kimmerer et al. 1994, Lehane & Davenport 2002, Maar et al. in press).

No pseudofeces were found in the experiments, suggesting that all copepods removed from the water were ingested by the mussels. In contrast, up to 12% of the copepod *Tigriopus brevicornis* (1.2 mm long) cleared by *Mytilus edulis* were expelled in pseudofeces at concentrations of 330 copepods l^{-1} (Davenport et al. 2000). They suggested a mussel can digest, over time, a threshold value of 12 copepods h^{-1}. This conflicts with the results from the present study, where adult *Acartia tonsa* were cleared at rates up to 85 ind. h^{-1}. The lower ingestion rate found by Davenport et al. (2000) may either be a result of their methods (mussels were fed copepods unnaturally using a pipette directed into the inhalant stream) or be related to size and nutritional differences between the 2 copepod species.

The mussels' filtration rate on *Rhodomonas salina* was significantly lower in experiments with early copepodites and adults compared with experiments with nauplii and no copepods. Davenport et al. (2000) observed that when mussels inhaled adult *Tigriopus brevicornis*, because of their size and appendages, they often touched the mussels' inhalant tentacles and thereby caused the mussels to immediately stop filtering and reduced their valve gape. Future research could utilize a video camera monitoring the mussels' inhalant siphons, thereby making it possible to observe the copepod–mussel interaction and the associated influence of turbulence and developmental stage.

The Danish estuary Limfjorden is the most important area for *Mytilus edulis* production in Denmark. Phytoplankton biomass in Limfjorden was on average 162 µg C l^{-1} from 2000 to 2005, and the zooplankton biomass was on average 85 µg C l^{-1} during the same period (MADS 2007). A previous modelling study showed that the potential contribution of heterotrophic plankton to the diet of *Mytilus edulis* varied from 17 to 34% during summer depending on the turbulence levels near the bottom (Maar et al. 2007). Hence, heterotrophic plankton may be a major contributor to the diet of mussels at high turbulence levels, a conclusion in agreement with our results. The present study emphasizes that future investigations should consider the functional triangle between mussel clearance rates, turbulence and copepod escape behaviors, including potential differences between species when studying the efficiency of benthic–pelagic coupling in coastal marine ecosystems. Further, knowledge of the food value of this potential carbon source to the mussels needs further examination.

Acknowledgements. Thanks to B. Søborg and J. E. N. Larsen for invaluable assistance in the laboratory. T. Kiørboe and H. U. Risgård are thanked for constructive comments on an earlier version of this manuscript. These experiments were supported by Managing Benthic Ecosystems (MaBenE) (grant EKV3-2001-00144), Danish National Research Council (grant no. 21-04-0391) and Regimeskift i Limfjorden (grant no. 3304-FVFP-060671-01). We also thank 2 anonymous reviewers for their valuable comments on this manuscript.

LITERATURE CITED

Azam F, Fenchel T, Field JG, Gray JS, Meyer-Reil LA, Thingstad F (1983) The ecological role of water-column microbes in the sea. Mar Ecol Prog Ser 10:257–263

Berg HC (1983) Random walks in biology. Princeton University Press, Princeton, NJ

Berggreen U, Hansen BW, Kiørboe T (1988) Food size spectra, ingestion and growth of the copepod *Acartia tonsa* during development: implications for determination of copepod production. Mar Biol 99:341–352

Broglio E, Johansson M, Jonsson PR (2001) Trophic interaction between copepods and ciliates: effects of prey swimming behavior on predation risk. Mar Ecol Prog Ser 220: 179–186

Buskey EJ, Hartline DK (2003) High-speed video analysis of the escape responses of the copepod *Acartia tonsa* to

shadows. Biol Bull 204:28–37
Cloern JE (1982) Does the benthos control phytoplankton biomass in South San Francisco Bay? Mar Ecol Prog Ser 9: 191–202
Davenport J, Smith RW, Packer M (2000) Mussels *Mytilus edulis*: significant consumers and destroyers of mesozooplankton. Mar Ecol Prog Ser 198:131–137
Gilbert OM, Buskey EJ (2005) Turbulence decreases the hydrodynamic predator sensing ability of the calanoid copepod *Acartia tonsa.* J Plankton Res 27:1067–1071
Green S, Visser AW, Titelman J, Kiørboe T (2003) Escape responses of copepod nauplii in the flow field of the blue mussel, *Mytilus edulis.* Mar Biol 142:727–733
Hansen PJ (1989) The red tide dinoflagellate *Alexandrium tamarense*: effects on behaviour and growth of a tintinnid ciliate. Mar Ecol Prog Ser 53:105–116
Horsted SJ, Nielsen TG, Riemann B, Pock-Steen J, Bjørnsen PK (1988) Regulation of zooplankton by suspension-feeding bivalves and fish in estuarine enclosures. Mar Ecol Prog Ser 48:217–224
Hwang JS, Strickler R (2001) Can copepods differentiate prey from predator hydromechanically? Zool Stud 40:1–6
Jonsson PR, Tiselius P (1990) Feeding behavior, prey detection and capture efficiency of the copepod *Acartia tonsa* feeding on planktonic ciliates. Mar Ecol Prog Ser 60:35–44
Kimmerer WJ, Gartside E, Orsi JJ (1994) Predation by an introduced clam as the likely cause of substantial declines in zooplankton of San Francisco Bay. Mar Ecol Prog Ser 113:81–93
Kim Wong C (1996) Response of copepods to hydromechanical stimuli. Crustaceana 69:853–859
Kiørboe T, Møhlenberg F (1981) Particle selection in suspension-feeding bivalves. Mar Ecol Prog Ser 5:291–296
Kiørboe T, Saiz E (1995) Planktivorous feeding in calm and turbulent environments with emphasis on copepods. Mar Ecol Prog Ser 122:135–145
Kiørboe T, Møhlenberg F, Nicolajsen H (1982) Grazing rate and gut clearance in the planktonic copepod *Centropages hamatus* (Lilljeborg) in relation to food concentration and temperature. Ophelia 21(2):181–194
Kiørboe T, Saiz E, Visser A (1999) Hydrodynamic signal perception in the copepod *Acartia tonsa*. Mar Ecol Prog Ser 179:97–111
Lehane C, Davenport J (2002) Ingestion of mesozooplankton by three species of bivalve; *Mytilus edulis, Cerastoderma edule* and *Aequipecten opercularis*. J Mar Biol Assoc UK 82:615–619
Lenz PH, Hartline DK, Davis AD (2000) The need for speed. I. Fast reactions and myelinated axons in copepods. J Comp Physiol [A] 186:337–345
Maar M, Nielsen TG, Stips A, Visse AW (2003) Microscale distribution of zooplankton in relation to turbulent diffusion. Limnol Oceanogr 48:1312–1325
Maar M, Nielsen TG, Bolding K, Burchard H, Visser AW (2007) Grazing effects of blue mussel *Mytilus edulis* on the pelagic food web under different turbulence conditions. Mar Ecol Prog Ser 339:199–213
Maar M, Nielsen TG, Petersen JK (2008) Depletion of plankton in a raft culture of *Mytilus galloprovincialis* in Ría de Vigo, NW Spain. II. Zooplankton. Aquat Biol 4:127–141
MADS (2007) Marine Database System. Available at: www.dmu.dk/Vand/Havmiljoe/MADS/
Newell CR, Wildish DJ, MacDonald BA (2001) The effects of velocity and seston concentration on the exhalant siphon area, valve gape and filtration rate of the mussel *Mytilus edulis.* J Exp Mar Biol Ecol 262:91–111
Nielsen TG, Maar M (2007) Impact of a blue mussel *Mytilus edulis* bed on vertical distribution and composition of the pelagic food web. Mar Ecol Prog Ser 339:185–198
O'Riordan CA, Monismith SG, Koseff JR (1995) The effect of bivalve excurrent jet dynamics on mass transfer in a benthic boundary layer. Limnol Oceanogr 40:330–344
Saiz E, Kiørboe T (1995) Predatory and suspension feeding of the copepod *Acartia tonsa* in turbulent environments. Mar Ecol Prog Ser 122:147–158
Støttrup JG, Richardson K, Kirkegaard E, Pihl NJ (1986) The cultivation of *Acartia tonsa* DANA for use as a live food source for marine fish larvae. Aquaculture 52:87–96
Titelman J, Kiørboe T (2003) Predator avoidance by nauplii. Mar Ecol Prog Ser 247:137–149
Verity PG, Smetacek V (1996) Organism life cycles, predation, and the structure of marine pelagic ecosystems. Mar Ecol Prog Ser 130:277–293
Visser AW (1997) Using random walk models to simulate the vertical distribution of particles in a turbulent water column. Mar Ecol Prog Ser 158:275–281
Waggett RJ, Buskey EJ (2007) Copepod escape behavior in non-turbulent and turbulent hydrodynamic regimes. Mar Ecol Prog Ser 334:193–198
Wong WH, Levinton JS, Twining BS, Fisher NS, Kelaher BP, Alt AK (2003) Assimilation of carbon from a rotifer by the mussels *Mytilus edulis* and *Perna viridis*: a potential food-web link. Mar Ecol Prog Ser 253:175–182

Editorial responsibility: Otto Kinne, Oldendorf/Luhe, Germany

Submitted: July 3, 2008; Accepted: October 27, 2008
Proofs received from author(s): February 3, 2009